Surface Analysis of Disbonded Titanium/Sol-Gel/Polyimide Joints

Jesse T. Cherian, David G. Castner, and Robert M. Fisher

(Submitted 18 March 2002; in revised form 3 June 2002)

Disbonded lap-shear specimens were analyzed to determine the locus of failure within bonded titanium (Ti) sol-gel polyimide joints. Bonded Ti alloys are being evaluated for use at an operating temperature of 175 °C. Determining the locus of failure for bonded Ti lap-shear specimens is part of a larger effort to develop durable, environmentally safe surface treatments for Ti alloys. Surface-treated Ti alloy (Ti-6Al-4V) plates are bonded in a standard lap-shear specimen configuration and exposed to temperature for specified intervals. The lap-shear bond joint consists of two etched Ti panels coated with a silicon and zirconium containing sol-gel, primed with a polyimide, and then bonded together with adhesive and supporting scrim material. The lap-shear specimens are tested for overall strength and failure modes. Specimens with adhesive failure modes were examined with x-ray photoelectron spectroscopy (XPS) to determine the composition of the bond joint failure layer. Analysis shows that the failure was located closer to the sol-gel/polyimide interface than to the Ti/sol-gel interface. Transmission electron micrographs (TEM) of the cross-sectioned joint confirmed the chemical distribution determined from the XPS data.

Keywords bonded titanium alloys, sol-gel coating, Ti-6Al-4V

1. Introduction

Structural adhesive systems are of interest to aircraft manufacturers since weight savings in aircraft design still continue to be an important way to improve profitability of aircraft. If the heavier metallic fasteners could be replaced with thin adhesive layers, the potential weight savings would be tremendous. In addition, the vision for a high-speed civil transport plane (HSCT) that would fly at supersonic speeds continues to light the imagination of industry and government alike. Supersonic aircraft flying at Mach 2.4 were expected to see temperatures as high as 175 °C at the leading edge. A sol-gel coating on titanium (Ti) produces an interface between the metal and organic resin with equivalent strength and environmental durability to the standard processes currently used, without generating significant hazardous wastes or using environmentally undesirable or toxic materials. Sol-gel processes are being developed for Ti that has mechanical properties equivalent to currently used processes, and with extended durability in a hot/wet environment.[1-3] The sol-gel is formed from a mixture of zirconium (Zr) isopropoxide and a silane in water. The current process produces coatings that vary from 100-2000 Å in thickness.

If such an aircraft were to be built, it would make use of as few fasteners as possible and would require the use of high temperature adhesives. These concepts motivated industrial research conducted at various governmental, academic, and industrial sites investigating a variety of pretreatment surface preparations and adhesive bonding systems. This research is born out of part of that effort.[4,5]

In the beginning of this work, an adhesive development program was created in part to evaluate the durability and strength of various adhesives systems used to bond several different Ti alloys. Various Ti alloys were used as substrates and bonded together in a standard, single lap-shear configuration.[6] After bonding, the specimens were tensile tested, and stress values were collected along with failure modes. Specimens that failed were characterized by visual inspection as primarily adhesive or cohesive failures. An adhesive failure was considered to be a failure that appeared to have broken away from the metal-oxide interface, while a cohesive failure was one that appeared to have broken down within the adhesive system. This investigation originated at this juncture. Many of the specimens that were thought to be adhesive failures, i.e., the disbonded surface appeared metallic, were submitted for surface analysis. While visual inspection showed a metallic surface, the following surface analysis investigations showed otherwise.

2. Theory

2.1 Mechanical Diffusion

To create a polymer-metallic joint, the two surfaces must be in intimate contact. For the polymer-metal interface to be formed, thermodynamic minimization of free energy at the surface must occur. Both physical and chemical interactions will undergo reduction of the available free energy of the interface as bonding occurs. To maximize the surface interface to have as many chemical bonds as possible, a surface roughening is desired. This is accomplished by creating a rough porous oxide on the metal surface. The porous oxide can easily accept

Jesse T. Cherian, Northwest Surface Laboratory and Department of Materials Science and Engineering, University of Washington, Seattle, WA 98195; **David G. Castner,** Department of Chemical Engineering, Box 351750, University of Washington, Seattle, WA 98195; and **Robert M. Fisher,** Lab/Cor, Inc. and Department of Materials Science and Engineering, University of Washington, Seattle, WA, 98195. Contact e-mail: jtcherian@nwsl.net.

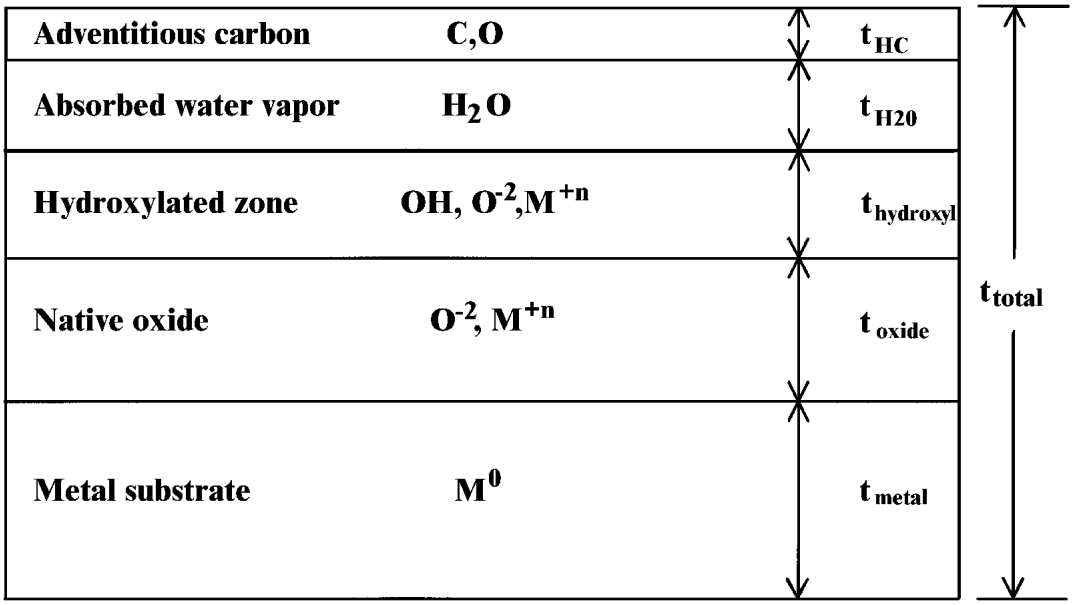

Fig. 1 Typical surface structure of Ti

a greater amount of polymer into its porous surface and increase the surface area in actual contact. Even with apparently smooth metal and cured polymer surfaces, the surface microstructure of both the metal and polymer contain asperities and voids in their respective surfaces that come into contact first. As these are slightly compressed together during the intimate contact while the adhesive bonding process occurs, the mechanical work put into creating the interface contributes to reducing voids and irregularities at the interface. As plastic deformation occurs locally at the asperity-asperity interface, or as the void closes, the dislocation energy is minimized. The work of adhesion model derived from the Young-Dupree equation governs the thermodynamic driving force for the energy minimization at the polymer-metal interface:

$$W_a = \gamma_{metal} + \gamma_{polymer} - \gamma_{polymer/metal}$$

In this equation W_a is defined as the work of adhesion, and γ_{metal}, $\gamma_{polymer}$, and $\gamma_{polymer/metal}$ are the free energies of each of the respective interface surfaces, denoted by the subscripts.[7,8] The mechanical or physical interaction is driven by the energy difference between the surfaces before the joint is formed and the interface after bonding. W_a must be greater than zero if the interface is to be stable.[9,10] This is the reversible work of adhesion that would have to be given up if the newly created polymer-metal interface were to be separated into the two original surfaces.

2.2 Chemical Bonding

Beyond the physical interaction at the polymer-metallic interface are the chemical reactions that may take place. The Ti metal substrates are generally received with the surface structure illustrated in Fig. 1.[11] The pretreatment process used to clean the surface of the Ti removes most of the t_{HC} exposing a relatively clean porous oxide structure that is covered with active hydroxyl sites. The surface oxides are further reacted with rinse water to form additional hydroxyl groups at the surface. The chemical bonding between the hydroxyl groups present on the Ti oxide surface and the silane structures from the sol-gel can be seen through the following hydrolysis and heterocondensation reactions.

APS (3-aminopropyltriethoxysilane) is mixed with TPOZ (tetra-n-propoxyzirconium, propanol), NH_4OH (ammonium hydroxide), $C_2H_4O_2$ (glacial acetic acid), and de-ionized water to form a sol. The APS and TPOZ are hydrolyzed as shown:

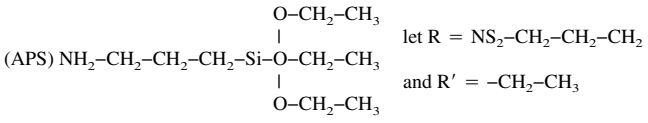

$$R–Si–(OR')_3 + 3H_2O \leftrightarrow R–Si–(OH)_3 + 3HO–R' \quad \text{(Eq 1)}$$

$$Zr–(OR'')_4 + 4H_2O \leftrightarrow Zr–(OH)_4 + 4HO\text{-}R'' \quad \text{(Eq 2)}$$

The condensation reaction is actually a hetero-condensation reaction that incorporates the hydroxyl groups on the Ti oxide surface.

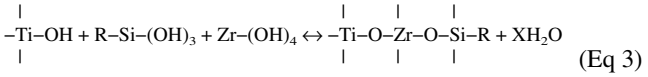

(Eq 3)

The sol-gel network that actually forms is three-dimensional. The strong M-O-M′ bonds that form are difficult to break, even at high temperatures. Blohowiak et al. suggested

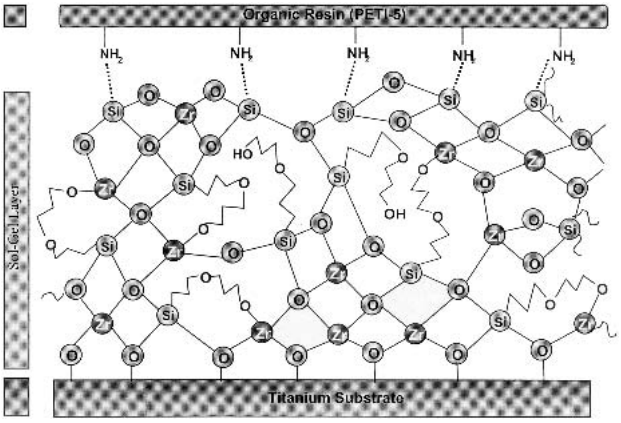

Fig. 2 Ti/sol-gel/polyimide interface

that the network should be arranged similar to Fig. 2.[2] The exposed surface of the sol-gel is expected to be rich in Si with Zr preferring the Ti interface. Hergenrother provided the structure for PETI-5 shown in Fig. 3.[12] The organic resin component is the polyimide primer identified as phenylene terminated imide oligomer (PETI-5). The trade name for the PETI-5 primer is BR®x5, a polyimide based adhesive (Cytec, Havre de Grace, MD). While the processing of PETI-5 is not part of this study, understanding the chemical structure is important for proper interpretation of the surface analysis data presented in later sections.

2.3 X-ray Photoelectron Spectroscopy

X-ray photoelectron spectroscopy (XPS) is also known as electron spectroscopy for chemical analysis (ESCA). The terms XPS and ESCA are interchangeable, and both are found throughout the literature.[13-15] The XPS analyses were performed at the Boeing Materials Technology (BMT) Surface Characterization Laboratory, Renton, WA and the University of Washington's Surface Analysis Recharge Center (SARC), Seattle, WA. The instruments at both facilities are Surface Science Laboratories SSX-100 generation spectrometers that used soft monochromatic Al Kα x-rays as a primary excitation source. The configuration at the SARC is an S-Probe while the BMT instrument is an M-Probe. This posed no problem for compatibility, as the calibrations for both instruments were equivalent.

The XPS experiment is illustrated in Fig. 4. An electron beam is directed at an anode producing x-rays directed at the solid sample being analyzed. This excitation energy $h\nu$, will produce a photoelectron as follows:

$$E_{KE} = h\nu - E_{BE} - \phi$$

where E_{KE} is the kinetic energy detected from the emitted photoelectron, E_{BE} is the binding energy of the electron in the solid, and ϕ is the work function. If the emitted electron escapes from the sample elastically without interacting with any neighboring particles, the electron's kinetic energy is undiminished and will appear as a peak rising above the background.

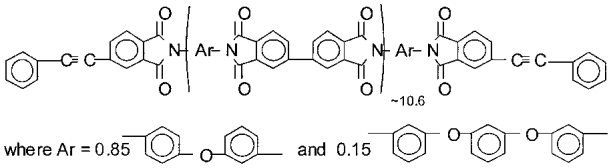

Fig. 3 PETI-5 (molecular weight of oligomer ~5,000 g/mol)

This background is created by the other emitted electrons that interact with the solid on their way out of the sample. These inelastic collisions can also appear as energy loss lines. XPS data is typically reported as the plot of the binding energies (calculated from measured E_{KE}) versus the total detected emission or counts (arbitrary units).

The emitted electrons are measured in a hemispherical energy analyzer at various pass energies. Lower pass energies (25-50 eV) are used for acquiring high resolution spectral when finer energy resolution is required for determining binding energy shift information. Higher pass energies (100-150 eV) are used for higher signal strength with some decrease in energy resolution but significant improvement in accuracy for quantification. The instruments detect the top 10-100 Å of a given surface in a circular or elliptical pattern that can be adjusted from 150-1000 μm. For nonconducting samples (PETI-5, SG), a low energy electron flood gun (<5.0 eV) is used to dissipate charging on the surface. In the case where the flood gun was used, the spectra were corrected by setting the hydrocarbon C (1*s*) peak at 285.0 eV as a binding energy reference and similarly adjusting the rest of the spectral lines. All analyses were conducted with a high vacuum environment with pressures lower than 1×10^{-8} torr.

XPS is used to determine the atomic composition of a given surface from the measured peak areas. Additionally the chemical functionality can be determined from the shifts in the binding energy for a given element. For example, the C (1*s*) line from C–C or C–H bonds found in polymers would be at 285.0 eV, while the same line from a CF2 bond would be found at 292.5 eV. Various peak-fitting algorithms are used to quantify the different peaks appearing in a multiple-peak spectrum. Atomic concentrations are calculated based upon the relative area under each peak after factoring in their photo-ionization cross sections.[16-19]

3. Experimental

3.1 Specimen Preparation

Thin Ti plates, nominally 100 × 150 × 1 mm, were used to fabricate standard lap-shear specimens. The Ti plates were first cleaned using a surface pretreatment, and then a sol-gel coating was applied. After a partial cure to initiate the hydrolysis-condensation reaction within the sol-gel coating, the surface was coated with a polyimide primer. Finally a polyimide adhesive was applied with a supporting fiberglass scrim and the lap-shear specimens were fully cured and bonded to form a strong joint. The pretreatment process used to remove oils, scale, and other surface contaminants also created a thin, porous oxide surface that covered with the active hydroxyl

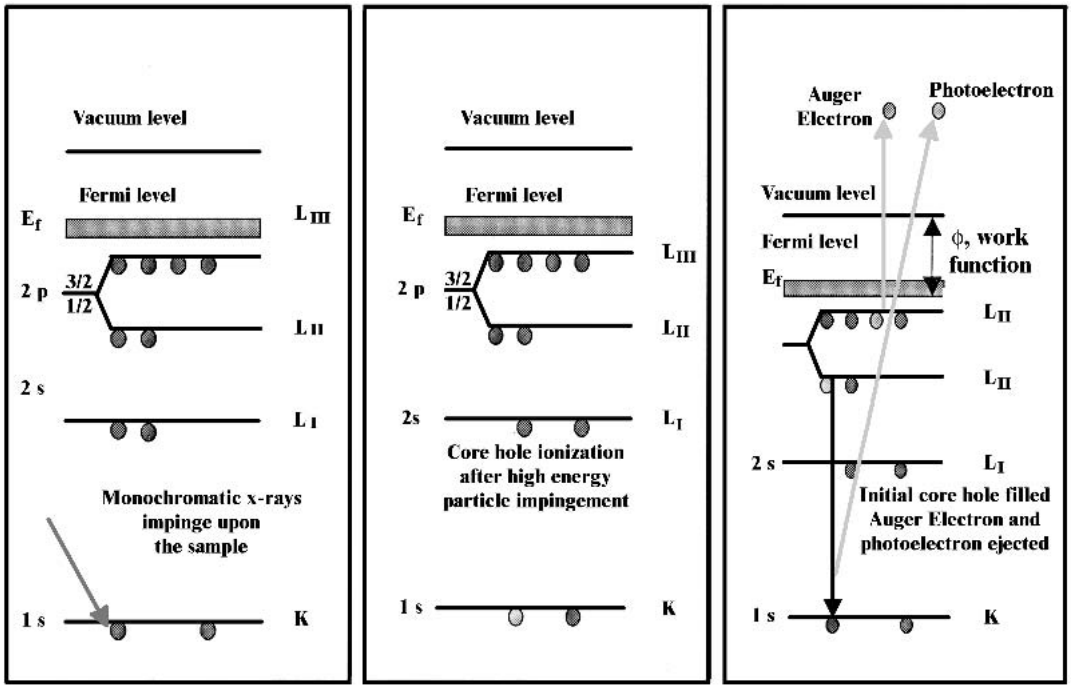

Auger Kinetic Energy

$$E_{KLL} = E_K - E_{LII} - E^*_{LII}$$

Einstein's Relation for Photon Energy

$$h\nu = E_{(KE + BE)}$$

Where h = Planck's Constant = 6.62×10^{-34} J s

ν = Frequency (Hz) of the radiation

Photoelectron Binding Energy

$$E_{KB} = h\nu - E_{BE} - \phi$$

Where ϕ = the work function of the spectrometer

Fig. 4 XPS (ESCA) process

groups shown previously in Fig. 1. These processes are all covered under various Boeing patents.[20-28]

3.2 Test Procedures

The bonded lap-shear specimens were tensile tested, and stress values were measured and categorized by specific failure modes. Specimens that failed were characterized by visual inspection and were designated by their failure mode as an adhesive or cohesive failure. An adhesive failure was one that appeared to have failed at the metal-oxide interface, while a cohesive failure was considered to be a failure inside the adhesive system. Many of the specimens that were thought to be adhesive failures, i.e., the disbonded surface appeared metallic, were submitted for surface analysis. A casual visual inspection showed a metallic surface. The surface chemistry determined from a thorough failure analysis investigation of the disbonded surfaces reveals what is not apparent from this initial visual inspection. XPS analysis was made in multiple regions within the zone thought to have failed adhesively. The drawing in Fig. 5 illustrates the bonding of the Ti plates and their subsequent separation and analysis zones. Additional analysis was made using bonded joints and polished thin-foil cross sections of the joint. These were examined by transmission electron

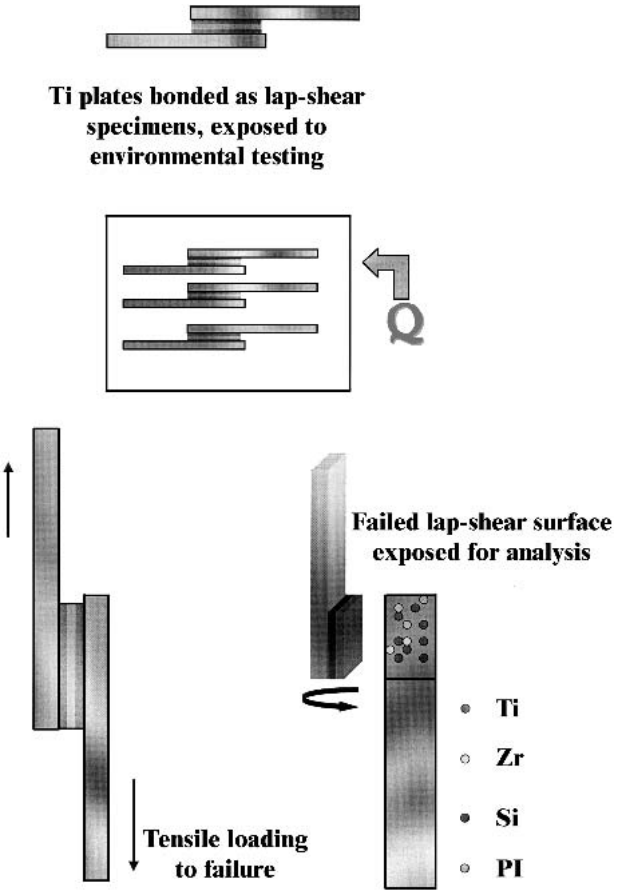

Fig. 5 Joint creation, testing, and analysis

microscopy (TEM) and probed with energy dispersive x-ray analysis. The concentration profiles were compared with the data obtained from the XPS analysis.

4. Discussion

Previous analysis determined that the sol-gel has distinct Si and Zr components. Since both Si and Zr are not native to Ti 6-4 or the polyimide primer, they are used as marker elements for the sol-gel coating. The metal substrate obviously has Ti as a marker, with no Si or Zr component. The primer layer, polyimide in nature would have C, O, and most notably N. Additionally, the high-resolution C (1*s*) spectra are well defined for polyimide and were also used as an identifying marker.[29] Analysis of mating surfaces in the zones where cohesive failure seemed to predominantly show polyimide on both sides of the exposed interface. In other instances, the failure clearly appeared to be within the sol-gel layer or an interphase layer. In these situations, the sol-gel marker elements of Si and Zr could be seen clearly on each mating surface of the failure, but no Ti or polyimide were in evidence. However, most of the analysis of the zones thought to have failed adhesively based upon the metallic appearance actually had components from the Ti substrate, the intermediate sol-gel layer, and the polyimide primer/adhesive. Multiple, consistent spectra were taken from

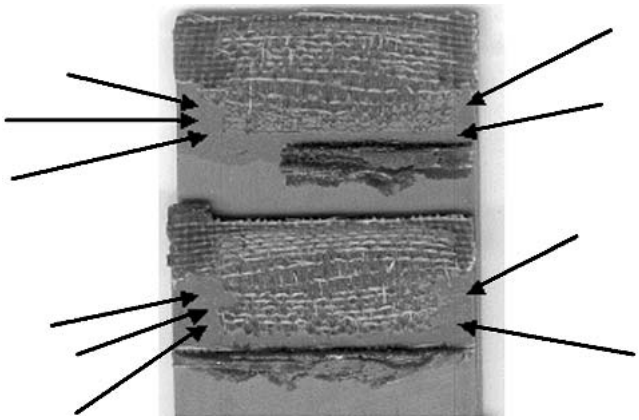

Fig. 6 Locations of XPS analysis on failed lap shear

each of the zones identified with arrows in Fig. 6. A typical spectrum from one of these regions (Fig. 7) shows a typical spectrum of this kind of failure. The spectra taken from these locations showed Ti signal from the native oxide layer on the substrate and also Si and Zr that clearly originate from the sol-gel layer. Figures 8 and 9 show the C (1*s*) and N (1*s*) high-resolution spectra indicating polyimide on the surface as well.

At first glance, one might conclude that the failure was not restricted to a discrete layer. The simultaneous signal of Ti, Si, Zr, and polyimide structure requires an explanation. However, a case for the failure to be, in fact, within a discrete layer can be made from the data. Comparing the theoretical Zr:Si ratios measured previously[3,30] and also understanding the depth of resolution available to the XPS instrument is essential to properly interpret the data. Consider the previous scanning electron microscopy (SEM) and Auger analysis that showed native Ti oxides on the order of 5-10 nm thick, while the sol-gel layer is measured much thicker at an average of 100 nm.[31] If the sol-gel forms into a complex Zr-Si network, as illustrated in Fig. 2, then the signal from the Zr would be weaker than the Si, and the Ti would be weaker still. The depth of resolution of XPS is nominally 10 nm or less, depending on the incident angle. If the failure occurred near the polyimide/sol-gel interface, the nearest Ti oxide would be 90 nm away, well beyond the depth of resolution of the XPS experiment. If the failure occurred near the Ti/sol-gel interface, then Ti signal would be much higher, and the Zr:Si ratio would be less than the theoretical mean for the material. In the bulk state, Zr:Si is approximately 1:6 or as high as 1:7. In the failed zones, the ratio increases four-fold to 1:28. The Zr-rich interface near the Ti substrate is buried under a thicker Si-rich zone with a polyimide layer masking most of the signal.

Besides the surface analysis efforts presented here, simultaneous microscopy efforts were coordinated at the University of Washington.[32] Using a Philips EM 430 (Eindhoven, The Netherlands) analytical transmission electron microscope (TEM), the micrograph in Fig. 10 was produced. Here a cross section of a bonded lap-shear joint shows that the sol-gel/oxide layer is quite a bit thicker than expected, measuring almost 400 nm. The difficulty in processing uniform bond lines is outside the scope of this study, but the micrograph illustrates the dif-

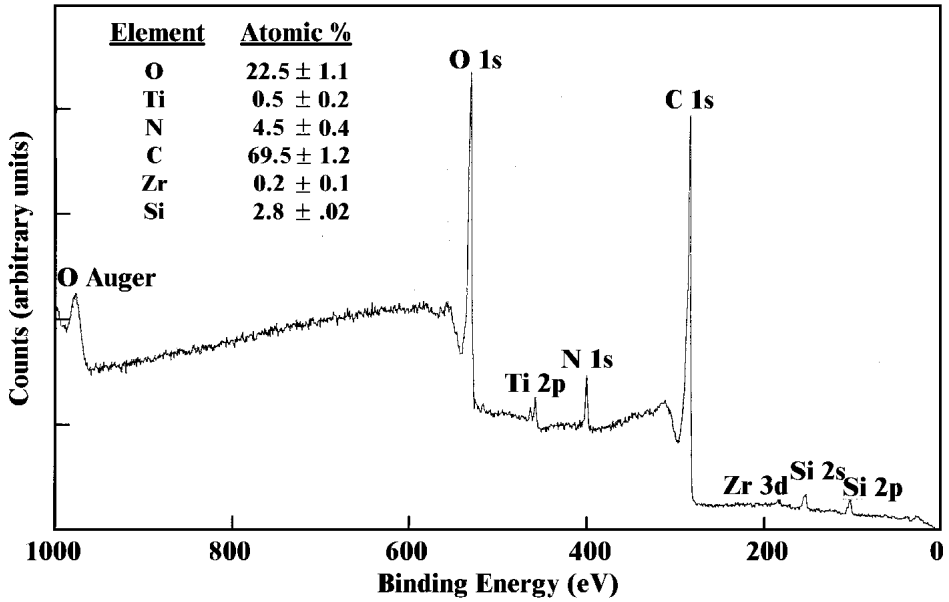

Fig. 7 XPS of failed lap shear specimen and average composition

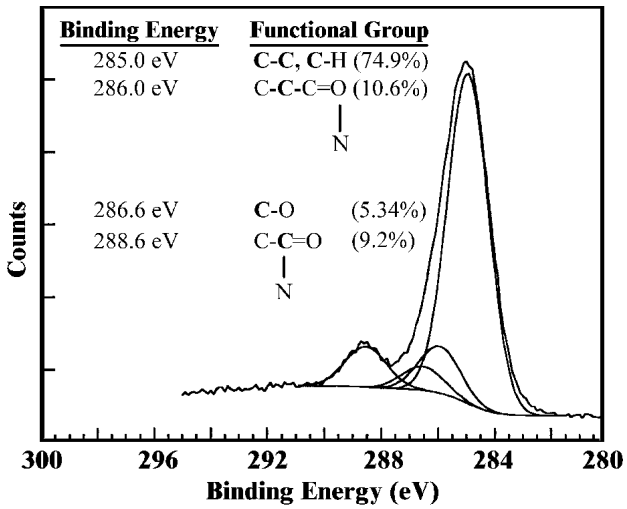

Fig. 8 High-resolution C (1*s*) photoelectron emission from failed lap-shear

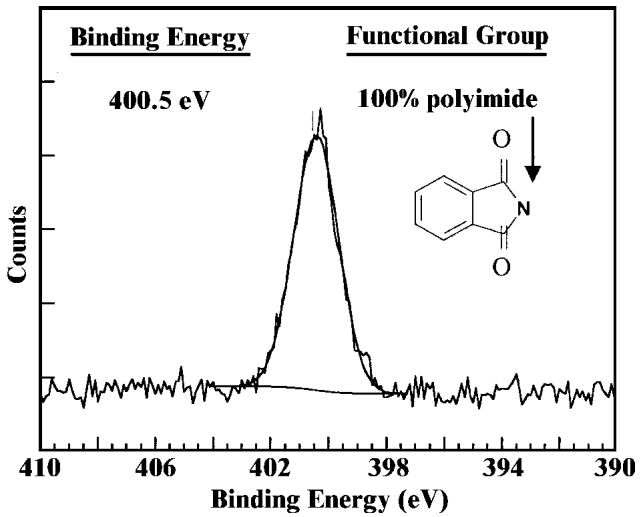

Fig. 9 High-resolution N (1*s*) photoelectron emission from failed lap-shear

ficulty of reproducing uniform bond lines. Energy dispersive x-ray microanalysis across the interface confirmed that Zr was concentrated at the Ti interface, while Si concentration increased near the polyimide interface. This is consistent with the interpretation of the XPS data and another indication that the theoretical model shown in Fig. 2 is accurate.

5. Concluding Remarks

The current interpretation is that the failure is, in fact, at the sol-gel/polyimide interface, more on the polyimide side. This would account for the strong polyimide structure and the trace amounts of marker elements from the sol-gel layer underneath the polyimide. The rough Ti oxide asperities occasionally push through the sol-gel/polyimide layer, giving rise to the trace amounts of Ti detected. There is a preferential orientation of Zr atoms near the Ti oxide interface, while the greater concentration of Si atoms is near the polyimide interface. Further analysis is being done using model systems that simulate the Ti sol-gel polyimide interface.

Acknowledgments

We would like to thank Kay Blohowiak and Kevin Pate at Boeing for their many contributions to this work. Kay's patience with the chemistry explanations and Kevin's outstanding program management enabled this research to occur. We also

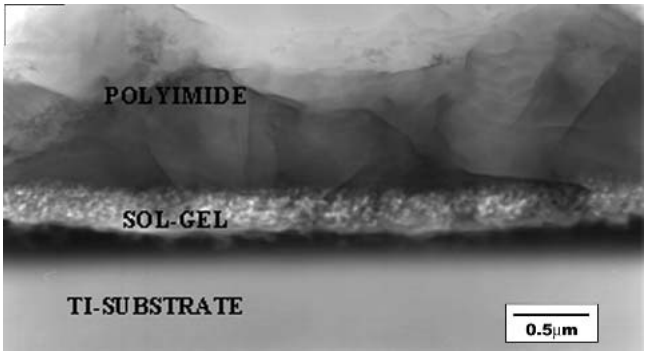

Fig. 10 TEM micrograph of the Ti 6-4/sol-gel/polyimide interface

acknowledge Paul Hergenrother at NASA for his PETI-5 diagrams. Finally, we are grateful to the management at Boeing Materials Technology and the SARC for the use of their facilities.

References

1. K.Y. Blohowiak, J.H. Osborne, K.A. Krienke, and D.F. Sekits: "Non-Chemical Surface Treatment for Titanium Alloys," Final Report Contract No. F33615-92-D-5812 (Wright Patterson Air Force Base, Wright Patterson, OH), Boeing, Seattle, WA, 1996.
2. K.Y. Blohowiak, K.A. Krienke, and D.F. Sekits: "Optimization and Scale-Up of Sol-Gel Technology for Preparation for Adhesive Bonding," Final Report Contract No. F33615-95-D-5615 (Wright Patterson Air Force Base, Wright Patterson, OH), Boeing, Seattle, WA, Feb 1997.
3. R.B. Greegor, K.Y. Blohowiak, J.H. Osborne, K.A. Krienke, J.T. Cherian, and F.W. Lytle: "X-Ray Spectroscopic Investigation of the Zr-Site in Thin Film Sol-Gel Surface Preparations," *J. Sol-Gel Sci. Technol.,* 2001, *20*(1), pp. 35-50.
4. K.D. Pate: "Materials Research for High Speed Civil Transport and Generic Hypersonics" in *Adhesives Development,* NAS1020220, Task No. 22, Subtask 3. National Aerospace and Space Administration, Hampton, VA, 1997.
5. J.E. Kurz and P.M. Hergenrother: "Airframe Materials and Structures, Composites, Adhesives, and Sealants," High Speed Research Program, Task No. 22 on NAS1- 20220, Industry Progress Report No. 27, Mar 1-31, 1998.
6. R.A. Kayless: Interfacial Chemistry and Adhesion: "The Role of Surface Analysis in the Design of Strong Stable Interfaces for Improved Adhesion and Durability," *Surf. Interface Anal.,* 1991, *17,* pp. 430-38.
7. G.A. Somorjai: *Introduction to Surface Chemistry and Catalysis,* John Wiley & Sons, New York, 1996, pp. 297-98
8. A. Furuya and Y. Ohshita: "Ti Concentration Effect on Adhesive Energy at Cu/TiW Interface," *J. Appl. Phys.,* 1998, *84*(9), pp. 4941-44.
9. B. Derby: "Metal Ceramics Interfaces" in *Diffusion Bonding, Acta Scripta Metallurgica,* Proceedings Series 4, H. Rühle, A.G. Evans, M.F. Ashby, and T.P. Hirth, ed., Pergamon Press, Oxford, UK, 1990, pp. 161-67.
10. E. McCafferty and J.P. Wightman: "An X-Ray Spectroscopy Sputter Profile Study of the Native Air-Formed Oxide Film on Titanium," *Appl. Surf. Sci.,* 1999, *143,* pp. 92-100.
11. E. McCafferty and J.P. Wightman: "Determination of the Concentration of Surface Hydroxyl Groups on Metal Oxide Films by a Quantitative XPS Method," *Surf. Interface Anal.,* 1998, *26,* pp. 549-64.
12. P.M. Hergenrother: private communication, 1999.
13. B.D. Ratner and D.G. Castner: "Electron Spectroscopy for Chemical Analysis" in *Surface Analysis-The Principle Techniques,* J.C. Vickerman, ed., John Wiley & Sons, New York, 1997, pp. 43-98,
14. D. Briggs and M.P. Seah: *Practical Surface Analysis by Auger and X-Ray Photoelectron Spectroscopy,* John Wiley & Sons, New York, 1983.
15. R.L. Chaney: "Recent Developments in Spatially Resolved ESCA," *Surf. Interface Anal.,* 1987, *10,* pp. 36-47.
16. D. Briggs: *Surface Analysis of Polymers by XPS and Static SIMS,* Cambridge University Press, New York, 1998.
17. G. Beamson and D. Briggs: *High Resolution XPS of Organic Polymers,* John Wiley & Sons, New York, 1992.
18. C.D. Wagner: "Auger and Photoelectron Energies and the Auger Parameter: A Data Set" in *Practical Surface Analysis,* D. Briggs and M.P. Seah, ed., John Wiley & Sons, New York, 1983.
19. J.M. Moulder, W.F. Stickle, P.E. Sobol, and K.D. Bomben: *Handbook of X-ray Photoelectron Spectroscopy,* Physical Electronics, Eden Prairie, MN, 1992.
20. K.Y. Blohowiak, J.H. Osborne, and K.A. Krienke: Surface pretreatment for Sol Coating of Metals, US Patent No. 5 869 141, 9 Feb 1999.
21. K.Y. Blohowiak, J.H. Osborne, and K.A. Krienke: Sol-Gel Coated Metal, US Patent No. 5 939 197, 17 Aug 1999.
22. K.Y. Blohowiak, J.H. Osborne, and K.A. Krienke: Surface Pretreatment of Metals to Activate the Surface for Sol-Gel Coating, US Patent No. 5 869 140, 9 Feb 1999.
23. K.Y. Blohowiak, J.H. Osborne, and K.A. Krienke: Sol Coating of Metals, US Patent No. 5 849 110, 15 Dec 1998.
24. K.Y. Blohowiak, J.H. Osborne, and K.A. Krienke: Sol for Coating Metals, US Patent No. 5 814 137, 29 Sept 1998.
25. K.Y. Blohowiak, J.H. Osborne, and K.A. Krienke: Hybrid Laminate Having Improved Metal-to-Resin Adhesion, US Patent No. 5 958 578, 28 Sept 1999.
26. K.Y. Blohowiak, J.H. Osborne, and K.A. Krienke: Chromate-Free Protective Coatings, US Patent No. 5 866 652, 2 Feb 1999.
27. K.D. Pate, "Sol-Gel Titanium Surface Treatment for Adhesive Bonding," HSCT-4-01, Revision E, The Boeing Company, Seattle, WA, 1998.
28. K.D. Pate: "Priming of Titanium with BR®x5 Primer," HSCT-4-04, The Boeing Company, Seattle, WA, 1996.
29. J.T. Cherian: Boeing HSCT Sol-Gel Specimen – 5000 Hours@400F, RT: Surface Analysis Via X-ray Photoelectron Spectroscopy, HSCT Titanium Surface Treatment Workshop, Renton, WA, Dec 9-10, 1997.
30. J.T. Cherian: "Practical Surface Analysis for Composites Manufacturing," MSE Thesis, University of Washington, Seattle, WA, 2000.
31. J.T. Cherian and G.A. Franck: "HSCT Lap-Shear Failure Analysis," Boeing Materials Technology W/R No. 98-00618, Renton, WA, 1997.
32. R.M. Fisher, J.T. Cherian, Z. Dai, and J. Holberry: "Surface Analysis and Characterization of Sol-Gel + PETI-5 Coatings on Ti 6-4," Final Report, NASA-Boeing HSCT Adhesive and Surface Treatment Program, University of Washington, Seattle, WA, 1998.